OPEN ACCESS Freely available online

PLOS ONE

Temperature Response of Soil Respiration in a Chinese Pine Plantation: Hysteresis and Seasonal vs. Diel Q_{10}

Xin Jia[1], Tianshan Zha[1]*, Bin Wu[1], Yuqing Zhang[1], Wenjing Chen[1], Xiaoping Wang[2], Haiqun Yu[2], Guimei He[2]

1 School of Soil and Water Conservation, Beijing Forestry University, Beijing, China, **2** Beijing Forestry Carbon Administration, Beijing, China

Abstract

Although the temperature response of soil respiration (R_s) has been studied extensively, several issues remain unresolved, including hysteresis in the R_s–temperature relationship and differences in the long- vs. short-term R_s sensitivity to temperature. Progress on these issues will contribute to reduced uncertainties in carbon cycle modeling. We monitored soil CO_2 efflux with an automated chamber system in a *Pinus tabulaeformis* plantation near Beijing throughout 2011. Soil temperature at 10-cm depth (T_s) exerted a strong control over R_s, with the annual temperature sensitivity (Q_{10}) and basal rate at 10°C (R_{s10}) being 2.76 and 1.40 μmol m^{-2} s^{-1}, respectively. Both R_s and short-term (i.e., daily) estimates of R_{s10} showed pronounced seasonal hysteresis with respect to T_s, with the efflux in the second half of the year being larger than that early in the season for a given temperature. The hysteresis may be associated with the confounding effects of microbial population dynamics and/or litter input. As a result, all of the applied regression models failed to yield unbiased estimates of R_s over the entire annual cycle. Lags between R_s and T_s were observed at the diel scale in the early and late growing season, but not in summer. The seasonality in these lags may be due to the use of a single T_s measurement depth, which failed to represent seasonal changes in the depth of CO_2 production. Daily estimates of Q_{10} averaged 2.04, smaller than the value obtained from the seasonal relationship. In addition, daily Q_{10} decreased with increasing T_s, which may contribute feedback to the climate system under global warming scenarios. The use of a fixed, universal Q_{10} is considered adequate when modeling annual carbon budgets across large spatial extents. In contrast, a seasonally-varying, environmentally-controlled Q_{10} should be used when short-term accuracy is required.

Citation: Jia X, Zha T, Wu B, Zhang Y, Chen W, et al. (2013) Temperature Response of Soil Respiration in a Chinese Pine Plantation: Hysteresis and Seasonal vs. Diel Q_{10}. PLoS ONE 8(2): e57858. doi:10.1371/journal.pone.0057858

Editor: Ben Bond-Lamberty, DOE Pacific Northwest National Laboratory, United States of America

Received September 9, 2012; **Accepted** January 28, 2013; **Published** February 28, 2013

Funding: This study was financially supported by the Beijing Forestry University Young Scientist Fund (BLX2011008), International Science and Technology Cooperation Program of China (2009DFA92900), and National Key Technology and Science Research and Development Program of China (2008BAD95B07). The funders had no role in study design, data collection and analysis, decision to publish, or preparation of the manuscript.

Competing Interests: The authors have declared that no competing interests exist.

* E-mail: tianshanzha@bjfu.edu.cn

Introduction

A global effort is underway to mitigate anthropogenic climate change through afforestation/reforestation, in hope of sequestering carbon in plantation ecosystems. At the global scale, afforestation is occurring at 2.8 million ha yr^{-1} 1]. Understanding the environmental controls on carbon dynamics in new plantations is crucial for projecting future global carbon budget and climate scenarios, and could aid in assessing the effectiveness of carbon-oriented management practices in forestry.

Soil-surface CO_2 efflux, commonly referred to as soil respiration (R_s), constitutes a major source of carbon release to the atmosphere, and accounts for more than two-thirds of annual ecosystem respiration (R_e) and one-half of gross ecosystem photosynthesis (P_g) in temperate forests 2]. Aside from its large quantity, R_s is exponentially related to soil temperature (T_s) in most ecosystems 3,4]. Consequently, even subtle changes in climate (e.g., rising atmospheric temperature) could trigger significant changes in R_s, markedly altering ecosystem carbon budgets. In turn, warming-induced increases in soil CO_2 emissions could feed back to the climate system, although the intensity of climate–carbon cycle feedbacks remains an issue of debate 5]. Despite the large body of literature on the interactions between R_s and climate change, the response of soil carbon processes to climatic factors (e.g., T_s and soil moisture) is not well-known and remains a source of uncertainty in ecosystem carbon modeling 6,7].

Soil CO_2 efflux is usually modeled as a simple function of T_s (e.g., the classic Q_{10} function) at both diel and seasonal scales 2]. However, under field conditions the response of R_s to T_s is modulated by multiple factors at multiple temporal scales 8,9]. An increasing body of evidence indicates that forest R_s is not adequately characterized by a simple function of T_s, as other regulators (e.g., microbial dynamics, plant phenology and photosynthesis, soil water content and soil porosity) are able to confound the R_s–T_s relationship and lead to hysteresis (or phase lags) in the R_s–T_s relationship at multiple scales 8–10]. Hysteresis relationships provide information on the causality between two processes 9]. Detecting and interpreting the decoupling between R_s and T_s over timescales of hours to seasons can provide important insights into the mechanisms driving R_s 9,10]. In addition, to accurately estimate carbon dynamics at multiple timescales in ecosystem carbon-cycle modeling, hysteresis relationships need to be explicitly considered 2,10]. The parameterization of R_s and R_e in carbon cycle models poses a major challenge when other factors confound the temperature response 7,11]. A recent synthesis

reported that hysteresis in the R_s–T_s relationship is more common in forests than previously recognized 9].

Apart from hysteresis, confounding factors also cause a discrepancy between long-term (e.g., annual) and short-term (e.g., diel) temperature response parameters (e.g., R_{s10}–the basal rate at 10°C; and Q_{10}–the temperature sensitivity) 2,11]. The apparent annual Q_{10} may not reflect the true biotic temperature sensitivity if obscured by seasonally varying factors other than T_s 11]. This is related to the ongoing debate on the use of a fixed (universal) vs. variable (environmentally-controlled) Q_{10} in carbon cycle modeling 7]. On the one hand, recent cross-site analyses point to a convergent sensitivity of respiration to temperature 7,12], negating previous conclusions that relate Q_{10} to climatic and substrate conditions 13,14]. Using FLUXNET data across 60 sites, Mahecha et al. 7] found that the apparent annual Q_{10} for R_e decreased with increasing mean annual temperature, while short-term Q_{10}, exempt from seasonally-confounding effects, converged to ~1.4 across sites. In addition, a meta-analysis revealed that the seasonal Q_{10} for R_s approximated 1.5 after excluding the confounding effects of vegetation seasonality 12]. On the other hand, single-site studies have reported large seasonal variation and temperature dependence of short-term unconfounded Q_{10} estimates for R_s in forest ecosystems 2,6,11]. Therefore, comparing longer-term, apparent Q_{10} estimates of seasonal sensitivity with shorter-term estimates of daily sensitivity may provide new insights into the driving mechanisms of R_s and R_e, and shed light on model parameterization.

Detecting hysteresis at multiple timescales and resolving the aforementioned debate require long-term measurements of R_s over both daily and seasonal cycles 15]. Recent studies have emphasized the use of automated chambers due to their ability to produce information about processes at fine temporal resolutions 16]. Continuous R_s measurements in China's plantation forests are rare, despite the country's extensive efforts in afforestation (e.g., 8.43 million ha of new plantations from 2004 to 2008) 1]. The few existing studies were mostly based on measurements made at coarse intervals (e.g., days to weeks) 17,18], which are inadequate to fully unravel the dependency of R_s on its controlling factors.

Using an automated chamber system, we monitored half-hourly values of R_s, T_s and soil volumetric water content (*VWC*) throughout 2011 in a Chinese pine (*Pinus tabulaeformis*) plantation at Badaling, about 50 km north of Beijing. Our objective was to quantify the seasonal and diel temperature responses of R_s. We asked: (1) whether R_s varies in-phase or out-of-phase with T_s at diel and seasonal timescales; and (2) whether the apparent annual Q_{10} and R_{s10} are consistent with values derived at the diel timescale. Within-stand spatial uncertainty was also analyzed and briefly discussed. We paid special attention to the implications of these results for the parameterization of carbon cycle models.

Materials and Methods

2.1. Ethics Statement

The study site is owned by Beijing Bureau of Forestry and Landscaping. The field work did not involve any endangered or protected species, and did not involve destructive sampling. Therefore, no specific permits were required for the described study.

2.2. Site description

The study site was a *P. tabulaeformis* plantation located in the Badaling Mountain region of Beijing (40°22.38'N, 115°56.65'E, 535 m a.s.l). The terrain is flat and uniform. The soil is of coarse-textured loess type, with phosphorous being the limiting nutrient for plant growth. The soil bulk density is 1.6 g cm^{-3}. The plantation was a stand of 4-year-old *P. tabulaeformis* trees with a mean diameter at breast height (*DBH*) of 3.2±0.8 cm (± standard deviation, SD) and a mean height of 2.2±0.3 m in May, 2011. The stand density was 975 stems ha^{-1}. The study site has no understory shrubs and only a sparse herbaceous cover (<10%).

The site is characterized by a temperate continental monsoon climate with hot and moist summers and cold and dry winters. Mean annual temperature (MAT) for 1985–2005 was 10.8°C, with highest and lowest mean monthly temperature of 26.9°C and −7.2°C in July and January, respectively (Meteorological Service of China). There were on average 160 frost-free days y^{-1}. Mean annual precipitation (MAP) was 454 mm, 59% of which fell in July and August. Mean annual potential evapotranspiration was 1586 mm, about three times the precipitation. The study year (2011) was cooler and wetter than normal, with MAT and MAP being 9.2°C and 568 mm, respectively.

2.3. Field measurements

An automated chamber system was installed at the study site in November 2010 to make half-hourly measurements of R_s. The system consisted of a LI-840 infrared gas analyzer (IRGA; LI-COR Inc., Lincoln, NE, USA), five custom-designed chambers, a CR1000 data logger (Campbell Scientific, Logan, UT, USA) and a rotary vane pump. Each chamber consisted of an alloy base and a moveable opaque dome. A pair of rotatable alloy arms connecting the dome and the base was promoted by a 12 V DC motor to open or close the chamber cap. When not in use, the chambers were kept open. The chamber base was placed over a fixed PVC collar which was 19 cm in diameter and 11 cm in height (inserted into the soil to a depth of about 7 cm). Collar insertion should have little impact on root dynamics because in this area most root biomass of *P. tabulaeformis* (>90%) is distributed at depths greater than 10 cm below the soil surface 19]. Rubber rings were used to seal the junctions among the chamber dome, base and collar. The tube connecting the chamber and the IRGA was about 15 m in length. The five chambers were randomly deployed in a 30-m diameter plot. A tube of 3 cm in length was mounted on the chamber as a vent to equalize the pressure inside and outside the chamber. Air temperature inside each chamber was measured using a type T thermocouple (Omega Engineering Inc., Stamford, CT, USA). The vegetation within collars was carefully removed one month before the start of measurements. Regrowth was minimal, and any regrowth was clipped regularly to avoid complication in the interpretation of the measurements.

The system measured soil CO_2 efflux at half-hourly intervals. Five chambers, which shared a common IRGA through a multiplexer, were activated one at a time in each measurement cycle. Prior to closure, each chamber was purged with ambient air for 2 min to flush out the tubing. After closure, the air was circulated through the chamber and IRGA at a flow rate of 0.5 L min^{-1}. The IRGA sampled CO_2 (μmol mol^{-1} moist air) and H_2O (mmol mol^{-1} moist air) concentrations over a 2 min interval, and the data logger recorded the mole fractions at 2 s intervals. The data logger computed the rate of change in CO_2 mixing ratio (μmol mol^{-1} dry air) through linear regression of the CO_2 mixing ratio against time (with a deadband of 10 s), and then calculated and stored the half-hourly rates of soil CO_2 efflux.

Half-hourly R_s (μmol m^{-2} s^{-1}) was computed as:

$$R_s = \frac{d\mathrm{CO}_2}{dt} \times \frac{PV}{ART} \quad (1)$$

where $d\mathrm{CO}_2/dt$ is the rate of change in CO_2 mixing ratio over time. P is the atmospheric pressure (atm). V is the chamber volume (L), which is the sum of the aboveground collar volume and the chamber-top volume. T is the air temperature within the chamber (K), A the soil area within the collar (0.028 m^2), and R the ideal gas constant (0.08206 L atm mol^{-1} K^{-1}). The chamber-top volume was 2.8 L for all chambers. Collar volumes were calculated for each sampling location through multiplying the aboveground collar height by A.

Half-hourly T_s and *VWC* at 10-cm depth were measured adjacent to each chamber. *VWC* was monitored with EC-5 soil moisture sensors (Decagon Devices Inc., Pullman, WA, USA) and T_s was monitored with thermistor probes (Omega Engineering Inc., Stamford, CT, USA). Each month, three soil cores of 3 cm in diameter to a depth of 15 cm were collected close to each chamber and stored in plastic bags. The 5–15 cm depth section of the soil samples were taken to the laboratory, weighed, oven dried at 80°C to constant weight, and reweighed to determine the gravimetric water content. Bulk density was determined for the same soil samples. Automated *VWC* measurements were then calibrated against those derived from manual measurements on a monthly basis.

2.4. Data analysis

The half-hourly CO_2 effluxes were screened as follows. Values outside the range of −5 to 20 μmol m^{-2} s^{-1} were considered abnormal and removed from the dataset. A mean ± 5SD criterion was then applied to monthly datasets to exclude outliers 1]. Instrument failure and quality control together resulted in 31% to 39% missing values for different chambers in 2011 (Fig. 1C). The remaining R_s data spanned the annual cycles of both T_s and *VWC*, allowing us to examine the relationships between R_s and its regulating factors. In order to estimate annual R_s, missing T_s values were gap-filled using empirical relationships to half-hourly soil temperatures recorded at an eddy-covariance tower 30 m away. When the tower measurements were also missing, the mean diurnal variation (MDV) method 20] with weekly windows was used to fill gaps in T_s.

The relationships between R_s and T_s were evaluated for both long-term (seasonal) and short-term (diel) timescales. The relationships were assessed for each sampling location separately, and also for the mean of the five chambers.

The long-term relationships were estimated based on daily mean values from complete annual cycle, using four common models: Exponential (Q_{10}) 21], Arrhenius 21], Quadratic 1] and Logistic 1] (see Table 1 for the equations). Daily mean rather than half-hourly values were used to minimize noise caused by asynchrony at the diel scale. Recent studies have shown that daily values are more robust than hourly values for examining seasonal responses to temperature 22]. The Q_{10} model was also fit separately for each month. Root mean square error (RMSE) and the coefficient of determination (R^2) were used to evaluate model performance. RMSE and R^2 were compared among models using a bootstrap approach in which the dataset was sampled 2000 times, followed by one-way analyses of variance (ANOVA) and Tukey's HSD multiple comparisons.

The short-term temperature response of R_s was quantified using half-hourly data. A single model (the Q_{10} function) was applied to a four-day moving window with a one-day time step. To minimize the effects of rain pulses and maximize the robustness of parameter estimation, observations during rainfall or within two hours after rainfall were excluded from the analysis, and a minimum R^2 of 0.5 was required for a valid regression.

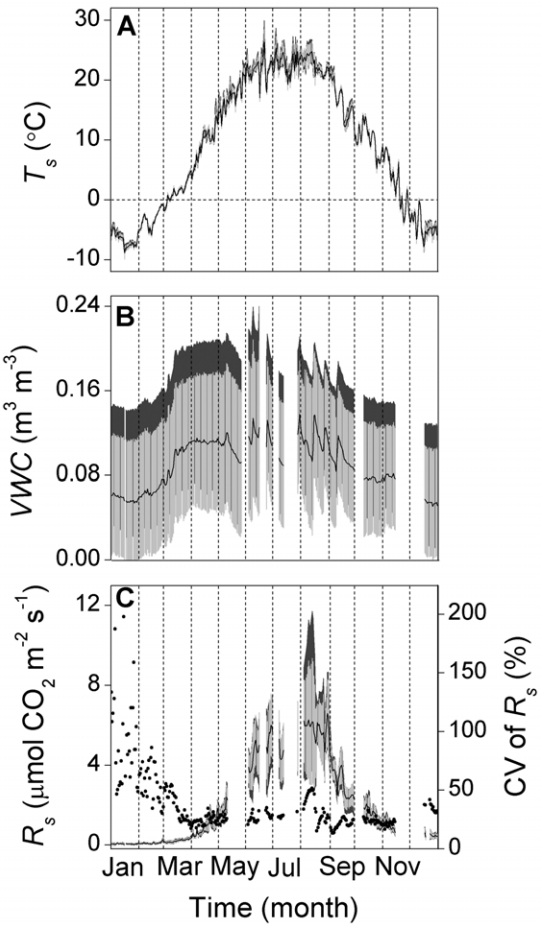

Figure 1. Soil temperature (T_s) (A), volumetric water content (*VWC*) (B) and soil respiration (R_s) (C). T_s and *VWC* were monitored at 10-cm depth. Solid lines: mean across measurement locations; light grey: standard deviation among measurement locations; dark grey: range among measurement locations; black dots in (C): coefficient of variation (CV) for R_s.
doi:10.1371/journal.pone.0057858.g001

Cross-correlation analysis was used to detect hysteresis between R_s and T_s at both the seasonal and diel timescales 9,23], and to synchronize the values before the regression was performed. In the case of seasonal hysteresis, analysis of covariance (ANCOVA) was used to examine the difference in R_s between the first (Jan–June) and second (July–Dec) half of the year, with T_s as the covariate. Values of R_s were log-transformed prior to ANCOVA to meet the assumptions of a normal distribution and linear correlation with the covariate. The range, SD and coefficient of variation (CV) were taken as indicators of spatial variability in R_s, R_{s10} and Q_{10}.

The monthly Q_{10} models were used to gap-fill daily mean R_s and estimate annual total R_s. The 95% confidence intervals (CI) for annual R_s were estimated by bootstrapping, in which the gap-filled daily mean R_s time series was sampled 2000 times. All analyses were processed in Matlab 7.11.0 (R2010b, The Mathworks Inc., Natick, MA, USA).

Table 1. Parameters and statistics for the analysis of the dependence of daily mean soil respiration (R_s) on soil temperature (T_s).

Location	Model	Adj. R^2	RMSE	R_{s10}/R_{s283}	Q_{10}	E_0
Spatial mean	Exponential	0.925[d]	0.567[d]	1.40	2.76	
	Arrhenius	0.929[c]	0.550[c]	1.40		70.99
	Quadratic	0.941[b]	0.503[b]			
	Logistic	**0.948**[a]	**0.473**[a]		4.27	
Location #1	Exponential	0.818[d]	0.535[d]	1.05	2.30	
	Arrhenius	0.821[c]	0.537[c]	1.06		57.27
	Quadratic	0.850[b]	0.486[b]			
	Logistic	**0.854**[a]	**0.486**[a]		3.47	
Location #2	Exponential	0.866[a]	1.058[a]	1.52	3.57	
	Arrhenius	0.867[a]	1.054[a]	1.51		88.76
	Quadratic	0.859[b]	1.087[b]			
	Logistic	**0.868**[a]	**1.052**[a]		4.01	
Location #3	Exponential	0.900[d]	0.731[d]	1.66	2.56	
	Arrhenius	0.907[c]	0.706[c]	1.66		65.66
	Quadratic	0.929[b]	0.615[b]			
	Logistic	**0.945**[a]	**0.544**[a]		4.91	
Location #4	Exponential	0.899[d]	0.528[d]	1.09	2.61	
	Arrhenius	0.905[c]	0.514[c]	1.09		67.39
	Quadratic	0.918[b]	0.477[b]			
	Logistic	**0.929**[a]	**0.443**[a]		4.52	
Location #5	Exponential	0.958[c]	0.394[c]	1.32	3.39	
	Arrhenius	0.960[b]	0.386[b]	1.31		84.81
	Quadratic	0.954[d]	0.413[d]			
	Logistic	**0.963**[a]	**0.371**[a]		3.93	

Exponential: $R_s = R_{s10} Q_{10}^{(T_s-10)/10}$; Arrhenius: $R_s = R_{s283}\exp(E_0/283.15R)(1-283.15/T_s)$; Quadratic: $R_s = b_1 + b_2 T_s + b_3 T_s^2$; Logistic: $R_s = \frac{b_1}{1+\exp(b_2(b_3-T_s))}$. T_s was measured at the 10 cm depth. R_{s10} and R_{s283}: basal rate of R_s at 10°C, in units of μmol m^{-2} s^{-1}; Q_{10}: relative increase in R_s for a 10°C increase in T_s; E_0: activation energy for R_s, in units of KJ mol^{-1}; R: universal gas constant (8.314 J mol^{-1} K^{-1}); b_1 through b_3: fitted parameters. Adj. R^2: adjusted coefficient of determination; RMSE: root mean square error, in units of μmol m^{-2} s^{-1}. Values in bold indicate best-fits according to Adj. R^2 and RMSE. Different letters following Adj. R^2 and RMSE indicate significant differences at the 0.05 level.

doi:10.1371/journal.pone.0057858.t001

Results

3.1. Seasonal pattern of R_s and its temperature response

Daily mean T_s was lowest on January 16th (−8.9°C), rose rapidly in February to June, remained high throughout summer (~25°C), and decreased after mid August (Fig. 1A). Daily mean *VWC* averaged across locations was low in winter and high during the growing season, ranging from 0.05 to 0.14 m^3 m^{-3} (Fig. 1B). Pulse dynamics in *VWC* were obvious from May through September (Fig. 1B). Daily mean R_s averaged across locations showed strong but asymmetric seasonality over the year (Fig. 1C). Daily mean R_s was lowest in January (<0.1 μmol m^{-2} s^{-1}), did not show remarkable increases until March, peaked in August (>6.0 μmol m^{-2} s^{-1}), and then decreased rapidly to ~0.5 μmol m^{-2} s^{-1} at the end of the year. Cross-correlation analyses revealed that, although the correlation between daily mean R_s and T_s was highest at zero lag for all locations, the correlation coefficient was strongly asymmetric about the zero lag, with negative lags (R_s lagging T_s) reducing the correlation coefficient much more rapidly than positive lags.

Spatial variability in R_s was substantial. The CV of daily R_s among chambers varied between 10% and 50% from March to December (Fig. 1C), averaging 28%. The large CV in January and February was caused by the near-zero magnitude of R_s. We did not find any evidence that the spatial variation in R_s was related to *VWC* or the distance to trees.

All four models of the seasonal R_s–T_s relationship performed well (Table 1). The three-parameter logistic model performed slightly better than the others, with consistently higher R^2 and lower RMSE. However, the annual model fits were unable to capture the pronounced seasonal hysteresis that was evident in the daily data, with R_s in the second half of the season being larger than that in the first half at a given T_s (Fig. 2). Significant seasonal hysteresis in the R_s–T_s relationship was observed for all sampling locations (and also for the spatial averages), with greater magnitudes for locations #1–3 than #4–5 (Fig. 2). As a result, the most commonly cited Q_{10} model and the best-fit logistic model both failed to yield unbiased R_s estimates over the entire annual cycle. The Q_{10} model captured daily R_s in autumn well, but overestimated R_s in spring (Fig. 3A). In contrast, the logistic model underestimated daily R_s in late autumn (Fig. 3B). The $R_{s\_modeled}$ vs. $R_{s\_measured}$ regression line significantly deviated from the 1 1 line according to the 95% CI for the slopes and intercepts (Fig. 3D, E). The estimation was greatly improved by fitting the Q_{10} model separately for each month (Fig. 3C). Monthly estimation enhanced the R^2 of the $R_{s\_modeled}$ vs. $R_{s\_measured}$ relationship, reduced the RMSE, and made the relationship closer to the 1 1 line (Fig. 3F). Temperature normalized R_s ($R_{s,N}$; the ratio of observed to modeled values) for both the annual best-fit logistic model and monthly Q_{10} models were independent of *VWC* (results not shown).

The annual Q_{10} obtained from the exponential model was 2.76, varying from 2.30 to 3.57 across locations (Table 1). The estimated annual R_s total, as calculated with monthly Q_{10} parameters and gap-filled T_s, was 838 (758, 921) g C m^{-2}. Across locations, annual R_s varied from 538 (492, 585) to 1032 (920, 1146) g C m^{-2}. The spatial uncertainty for annual R_s was ±250 g C m^{-2}, estimated as the 95% CI for $n = 5$ locations, assuming a t distribution with $n-1$ degrees of freedom and $\alpha = 0.05$.

3.2. Diel temperature response of R_s

Both diel estimates of R_{s10} and Q_{10} showed strong seasonal trends (Fig. 4). Only the period from March to November is shown, as R_s values were so small and T_s oscillated so weakly in winter that the regressions produced unreasonable parameter estimates. Mean R_{s10} across locations was <1.0 μmol m^{-2} s^{-1} in early March, increased throughout April to June, peaked in early August (~4.5 μmol m^{-2} s^{-1}), and then decreased to ~1.50 μmol m^{-2} s^{-1} in November (Fig. 4A). Q_{10} was generally low in summer (1.5–2.0), but high at both ends of the growing season (2.0–4.0) (Fig. 4B). A peak in Q_{10} was evident between March and April.

The variability of R_{s10} and Q_{10} across locations can be quantified as functions of their magnitudes (robust regression with bisquare weights: *Range*_$R_{s10} = 0.73$ R_{s10}–0.17, $R^2 = 0.90$; *Range*_$Q_{10} = 0.82$ Q_{10}–0.47, $R^2 = 0.78$). Both daily R_{s10} and Q_{10} had CV values of between 0% and 50% for most time of the season, with high values of these parameters showing greater CV (Fig. 4A, B).

Daily R_{s10} was positively correlated with T_s, but with strong hysteresis (Fig. 5A). Fitting an exponential function of T_s to the spring and autumn seasons separately explained more than 80% of the seasonal variation in R_{s10}. Daily Q_{10} was negatively correlated

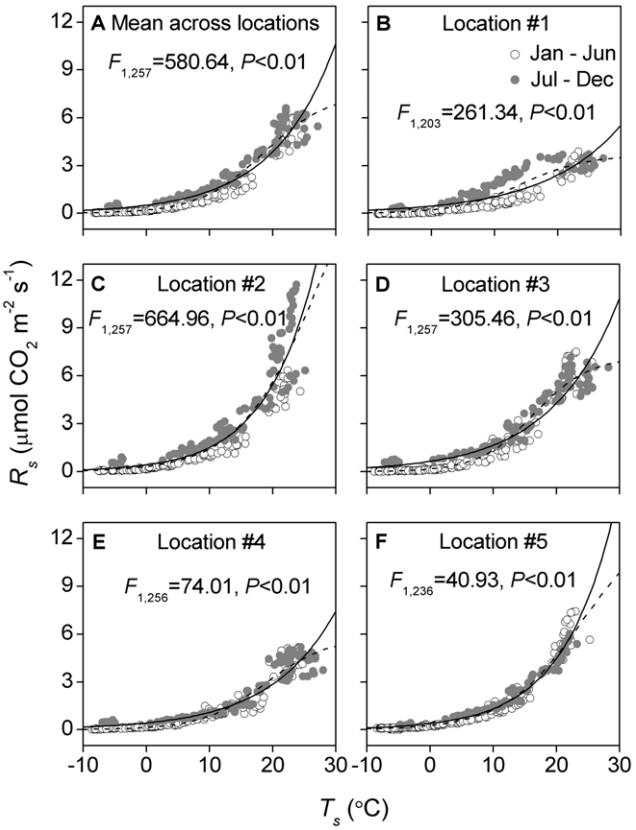

Figure 2. Relationships between daily mean soil respiration (R_s) and soil temperature (T_s). T_s was monitored at 10-cm depth. Open circles are from January to June; closed circles are from July to December. The solid lines are fitted by a Q_{10} model; the dashed lines are fitted by a logistic model. R_s is significantly different between the first and second half of the year when the *F*-test gives $P<0.05$.
doi:10.1371/journal.pone.0057858.g002

with T_s (Fig. 5B). An exponential function of T_s accounted for 59% of the seasonal variation in Q_{10}, with a decay rate constant of 0.04.

The lag between diel oscillations in R_s and T_s showed a strong seasonal pattern, with almost no lag in summer but lags up to five hours in the early and late growing season (Fig. 4C). In March and October, T_s reached its daily minimum at 08:00 and peaked at around 15:00 (Fig. 6A, C). In March R_s was out-of-phase with T_s, reaching its daily maximum at 11:00–14:00 and daily minimum at 19:00. In October, R_s was also out-of-phase with T_s, peaking at around 12:00 and reaching a minimum at around 24:00. The lags in March and October led to hysteresis loops (Fig. 6D, F), and the correlation between R_s and T_s was strongest after lagging R_s by three hours (Fig. 6G, I). In contrast, R_s was in phase with T_s in June (Fig. 6B, E), with the zero lag generating the highest correlation coefficient (Fig. 6H).

Discussion

4.1. Temporal pattern of R_s and hysteresis

Although the annual models fit the temperature response of R_s reasonably well, they all failed to capture the seasonal dynamics of R_s without bias over the annual cycle (Fig. 2, 3). This was due to the existence of seasonal hysteresis in the R_s–T_s relationship, which resulted in R_s being greater in the second than the first half of the year for a given T_s (Fig. 2). Hysteresis in the seasonal R_s–T_s relationship has been reported for various ecosystem types spanning a broad spectrum of climatic conditions, with the nature and magnitude of hysteresis varying across sites and vegetation types 8,9,24]. The decoupling of R_s from T_s is usually attributed to factors that confound the temperature effect. For example, Gaumont-Guay et al. 2] reported that a severe autumn drought caused seasonal hysteresis in the R_s–T_s relationship, leading to smaller R_s in autumn than in spring for a given temperature. Biotic factors that may confound the R_s–T_s relationship include plant photosynthesis, root growth, litterfall dynamics and microbial dynamics 2,9,11]. These factors affect the timing and magnitude of different R_s components, each of which can respond distinctly to T_s 25,26]. The observed hysteresis in this study, i.e., with higher R_s in the autumn than spring for a given T_s, was in agreement with several previous studies 24,27,28]. The spring-autumn differences can result from increased soil microbial activity during late summer in response to the warming of deeper soil layers 2], or from the accumulation of fresh litter and/or respiring biomass (e.g. microbes and roots) as the season proceeded 4].

Soil moisture has been reported to regulate the seasonal temperature response of R_s, e.g., Q_{10} decreases during drought 29]. However, we did not find any effect of soil *VWC* on R_s. A lack of regulation of R_s by soil moisture has also been reported for temperate and boreal coniferous forests 9,23]. The relatively low *VWC* values (0.05–0.14 m^3 m^{-3}), which reflect the high evapotranspiration, low soil water holding capacity and good drainage, may help explain the absence of *VWC* effect on R_s. Moreover, soil moisture impacts on R_s have been most commonly observed in arid or Mediterranean ecosystems, where hot and dry periods are common, during which T_s and *VWC* are negatively correlated 9,29]. The temperate continental monsoon climate at our site features high summer precipitation (~85% of the annual total fell from June to September in 2011), leading to a strong positive correlation between T_s and *VWC* ($r = 0.79$; $P<0.01$) and providing adequate water for high rates of root and microbial metabolism. Despite the drought in winter, the concurrent low temperatures and thermal limitation may have cancelled the restriction of R_s by low soil water (Fig. 1). Further investigation is needed to corroborate our conclusion on the role of *VWC* due to data gaps in summer (Fig. 1B, C).

We also observed diel lags in the R_s–T_s relationship (Fig. 4C, 6). Diurnal hysteresis has been quantified and modeled in various forest ecosystems, and was shown to either arise from the mismatch between the depth of temperature measurements and that of CO_2 production, or the regulation of diurnal R_s by the photosynthetic carbon supply 10,16]. More intriguingly, we found that the diurnal lag between R_s and T_s varied dramatically over the season; R_s and T_s were in-phase in summer, but T_s lagged R_s by about three hours in the early and late growing season (Fig. 4C, 6). Vargas et al. 16] also reported that the lag between hourly soil CO_2 production and T_s varied each day, showing that there is not a constant diel lag for each vegetation type. Seasonal changes in the diurnal lag as observed in our study may be the combined result of a varying depth of CO_2 production over the season and a constant reference T_s depth of 10 cm, i.e., with production at superficial layers in spring and autumn, and at deeper layers in summer. The primary depth of CO_2 production may vary seasonally in association with changes in the relative contributions of autotrophic *vs.* heterotrophic respiration 23], as these components often occur at different depths (e.g., shallow litter and soil organic matter decomposition and deep root metabolism). The observed diel R_s–T_s lags in March and October were unlikely caused by diel variations in photosynthetic carbon supply because most studies demonstrate a higher autotrophic contribution to R_s in the main growing season when plants are physiologically most

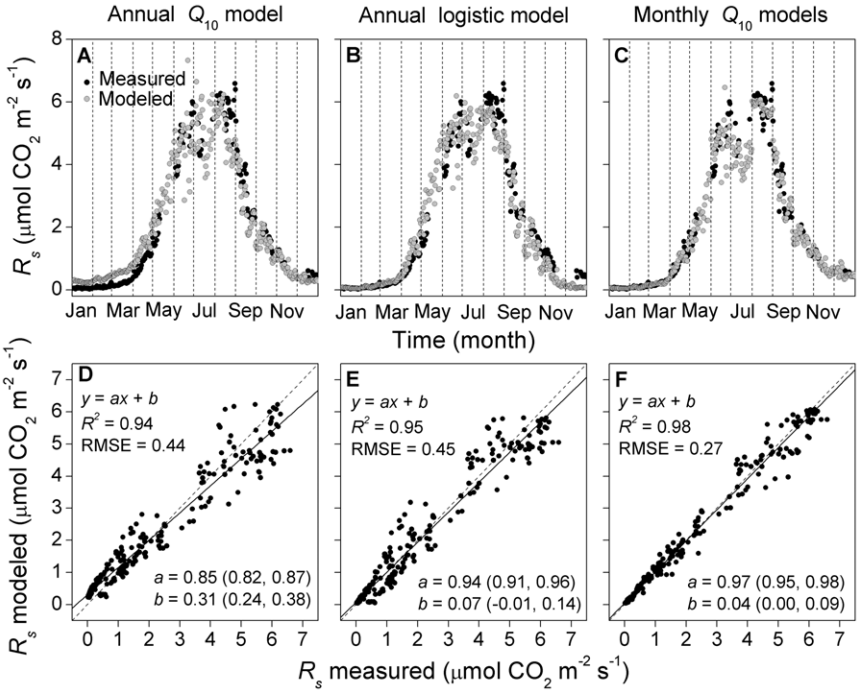

Figure 3. Comparisons between measured and modeled daily mean soil respiration (R_s). Modeled R_s values were derived from (A and D) an annual Q_{10} model, (B and E) an annual logistic model, or (C and F) monthly Q_{10} models. Values in parentheses in (D–F) represent 95% confidence intervals.
doi:10.1371/journal.pone.0057858.g003

active 23]. In addition, eddy-covariance measurements at our site revealed that ecosystem photosynthesis began in early May and ended in mid October, 2011 (unpublished data), and thus photosynthetic carbon supply was of little relevance to R_s in March and October.

4.2. Long- vs. short-term temperature response

The short-term temperature response of R_s (e.g. over the diel cycle) can deviate significantly from that for complete annual cycles because of seasonally-varying biophysical drives (e.g., root dynamics, plant photosynthesis) that confound the relationship of R_s with temperature 2,4,11]. In this study, average daily R_{s10} (1.89) and Q_{10} (2.04) were higher and lower, respectively, than those obtained from the seasonal relationship (2.76 and 1.40 μmol m^{-2} s^{-1} respectively, Table 1 and Fig. 4A, B). High rates of plant photosynthesis and microbial metabolism in summer are supposed to enhance summer R_s in addition to T_s, causing a higher apparent annual Q_{10} 2,23,30]. In contrast, Q_{10} calculated from the short-term or high-frequency temperature response is exempt from seasonally confounding effects, and thus better reflects the biological sensitivity of respiration to temperature 6,7,11]. Diel Q_{10} exhibited large seasonal changes and decreased with increasing T_s (Fig. 5B), which was consistent with many previous studies 2,6,11]. The reduction in Q_{10} with increasing T_s may be associated with the transition from acclimation of enzymatic activity at low temperatures to limitation by substrate supply at high temperatures 2,31]. A peak of Q_{10} was obvious at the start of the growing season (Fig. 4B), and may reflect a jump in root activity and associated respiration 3]; some studies have demonstrated that autotrophic respiration is more sensitive than microbial respiration to temperature, with the qualification that these studies were based on seasonal rather than short-term responses 23,25,32].

A caveat should be noted when interpreting the dependence of short-term Q_{10} on temperature. Because the amplitude of T_s oscillations dampens with depth in the soil profile, the decoupling of T_s measurement depth from CO_2 production depth may bias the estimation of temperature sensitivity 2,10]. The result will be an overestimation of Q_{10} when respiration occurs mostly above the temperature sensor (e.g., in the early and late growing season at our site), and an underestimation of Q_{10} when respiration occurs mostly below the temperature sensor. Therefore, the Q_{10}–T_s relationship in Fig. 5 might be partially explained by the dominance of shallow soil organic matter and litter decomposition (<10 cm) at both ends of the growing season when T_s is low. Experiments incorporating multi-layer T_s measurements or using the flux-gradient approach are needed to further assess the intrinsic relationship between Q_{10} and T_s.

The large seasonal variation in the diel estimates of R_{s10} reported here was in accordance with existing results from forest studies 2,4], and was responsible for the discrepancy between the larger apparent annual Q_{10} and the smaller short-term Q_{10} estimates. The asymmetric seasonal pattern of R_{s10} resulted in a clear hysteresis relationship between R_{s10} and T_s (Fig. 4A, 5A), which was similar to the mixed temperate forest study of Sampson et al. 4]. Instead of largely controlled by T_s of R_s, R_{s10} is usually an indicator of phenology, substrate supply, respiring biomass and the activity of roots and microbes 1,4]. The decoupling of daily R_{s10} from T_s was responsible for the seasonal hysteresis relationships between R_s and T_s observed in this study (Fig. 2).

4.3. Spatial uncertainty of R_s

Our results showed variations in the CV of R_s among locations, ranging from 10% to 50% (Fig. 1C). These values are comparable to those found in an oak-grass savanna where the spatial heterogeneity in vegetation cover was much higher 33]. In a *Picea*

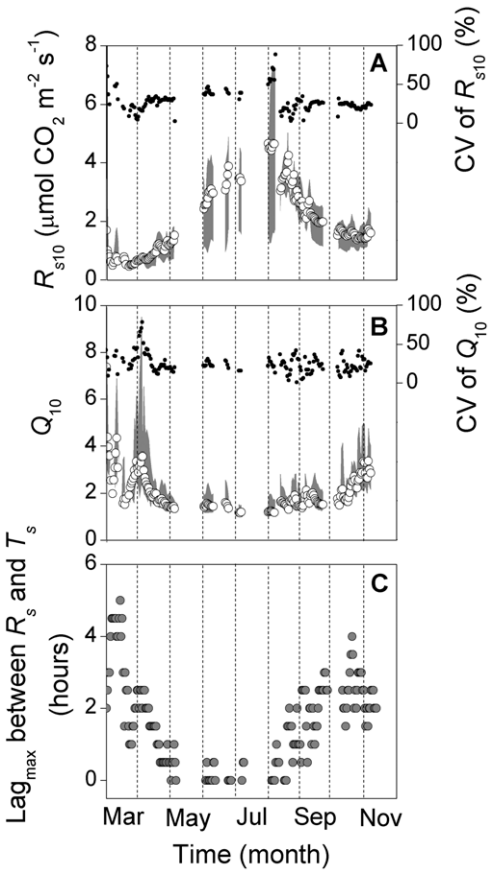

Figure 4. Daily R_{s10} (A), daily Q_{10} (B) and diel lags (lag_{max}) (C). R_{s10} refers to the basal rate of soil respiration at 10°C. Lag_{max} indicates the temporal lag that maximizes the correlation between soil respiration (R_s) and 10-cm soil temperature (T_s) over the diel cycle. Circles in (A–C): mean across measurement locations; grey area in (A and B): range among measurement locations; black dots in (A and B): coefficients of variation (CV) for R_{s10} and Q_{10}, respectively.
doi:10.1371/journal.pone.0057858.g004

abies stand, Buchmann 34] found that within-site variations of R_s had a CV of 40%. Adachi et al. 35] reported CV of ~40% for R_s in two subtropical plantations. The mean annual R_s of 838 g C m^{-2} from this study was greater than that found by Yu et al. 1] in a 50-year-old *Platycladus orientalis* plantation in Beijing (645 g C m^{-2}). This discrepancy may arise from the different stand ages and the recent disturbance of the soil by afforestation at our site. Estimated annual R_s at our site ranged from 538 to 1032 g C m^{-2}, with a spatial uncertainty of ±250 g C m^{-2}. Tang and Baldocchi 33] reported that the annual R_s was 394 g C m^{-2} in the open area and 616 g C m^{-2} under trees in an oak-grass savanna. Davidson et al. 36] reported annual R_s from a temperate mixed hardwood forest that ranged from 530 g C m^{-2} at the swamp site to 850 g C m^{-2} in a well-drained site. Therefore, the relatively uniform plantation we monitored exhibited R_s that had comparable spatial variability to that in more heterogeneous stands, probably the consequence of high spatial variability in its biophysical factors 3,29]. The required number of measurement locations for estimating annual R_s with error limits of 10% and 20% at our site was 45 and 11, respectively, calculated using the equation in 35].

Temperature response parameters also showed pronounced spatial variations (Fig. 2, 4A, B). The seasonal Q_{10} ranged spatially from 2.30 to 3.57; the daily Q_{10} showed CV values in the range of 0–50%. Xu and Qi 3] reported that the seasonal Q_{10} ranged spatially from 1.21 to 2.63 in a young ponderosa plantation in California, with a CV of larger than 20%. These results indicate that a spatially averaged Q_{10} may not be indicative of the sensitivity of R_s to temperature in an ecosystem 3].

4.4. Conclusions and implications for carbon modeling

This study's main findings are: (1) despite a strong temperature control on R_s, both R_s and short-term estimates of R_{s10} showed pronounced seasonal hysteresis with respect to T_s measured at 10-cm depth; (2) lags between R_s and T_s were observed at the diel timescale, but only in the early and late growing season; (3) the apparent annual Q_{10} (2.76) was larger than the mean daily Q_{10} (2.04), and daily Q_{10} decreased with increasing temperature. As detailed below, these findings have important implications for ecosystem carbon-cycle modeling.

Debate continues on the use of an invariant vs. biophysically-controlled temperature sensitivity to simulate respiration in carbon cycle models 6,7]. Some authors discovered that after ruling out seasonally confounding factors, convergent seasonal Q_{10} values (e.g., 1.4) emerged across sites spanning a diversity of climatic and vegetation conditions 7,12]. These studies negate previous conclusions relating Q_{10} to climate conditions 13,14] and argue for the use of a universal Q_{10} in modeling ecosystem respiration. In contrast, single-site continuous measurements have revealed large seasonal changes and environmental controls (e.g., soil tempera-

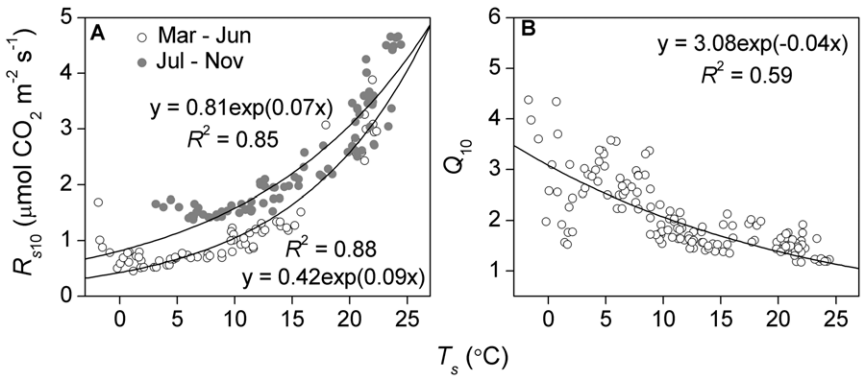

Figure 5. Relationships between soil temperature (T_s) and (A) daily R_{s10} and (B) daily Q_{10}. Open circles in (A) are from March to June, closed circles are from July to November.
doi:10.1371/journal.pone.0057858.g005

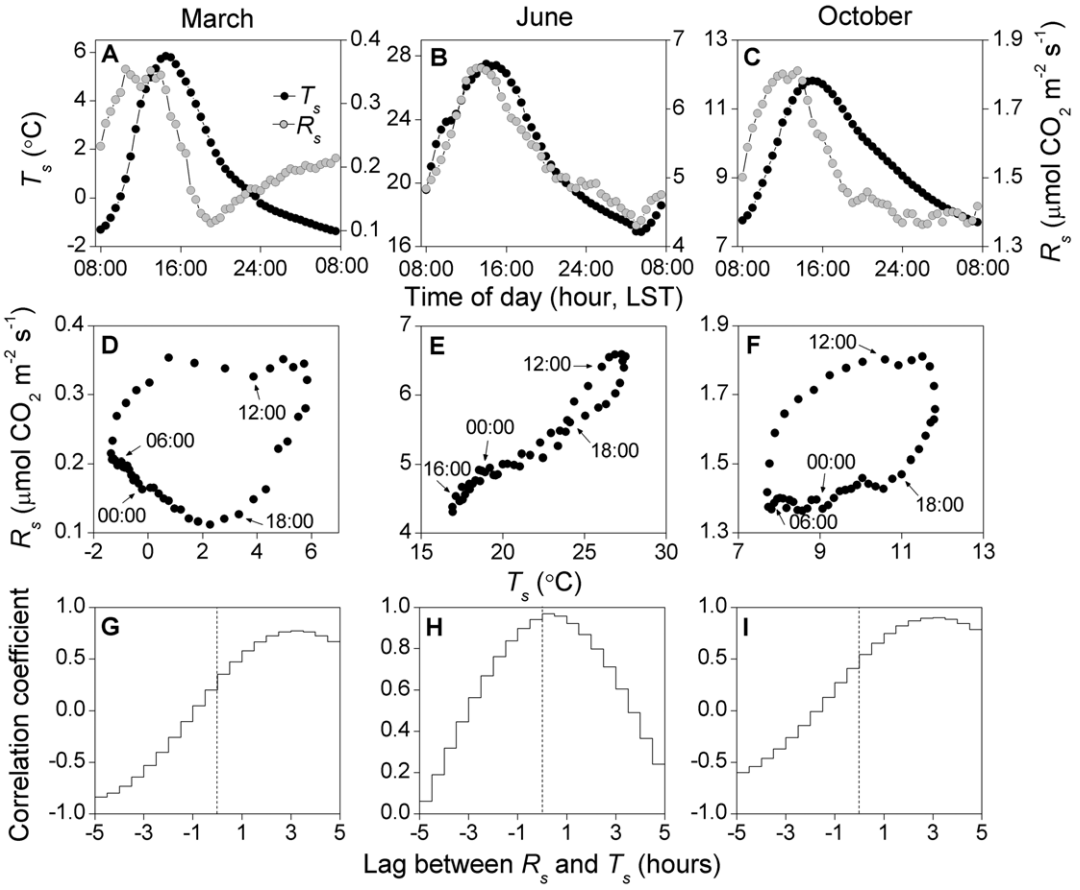

Figure 6. Diel soil respiration (R_s) and temperature (T_s) (A–C), diel R_s vs. T_s (D–I), their lag correlations (G–I). Mean values for March, June and October are shown. Grey circles in (A–C): R_s; Black circles in (A–C): T_s. T_s was monitored at 10-cm depth. The dashed lines in (G–I) are reference lines for the zero lag.
doi:10.1371/journal.pone.0057858.g006

ture and moisture, substrate supply) on short-term unconfounded estimates of Q_{10} 2,6,11]. Our results add support to the latter finding, showing a clear dependence of daily Q_{10} on temperature over the growing season.

We propose, however, that the convergent seasonal Q_{10} and the seasonally-varying short-term Q_{10} are not necessarily in contradiction with each other, because they both exclude seasonally confounding effects. Both of them, therefore, reflect an unconfounded sensitivity to temperature, albeit at different temporal and spatial scales. The use of a constant vs. variable, environmentally-controlled Q_{10} in a carbon cycle model then becomes a matter of the scale on which carbon fluxes are simulated. A fixed annual Q_{10} is considered adequate when the model aims to predict annual carbon budgets at large spatial extents across climatic zones and ecosystem types 7]. In contrast, environmental controls on Q_{10} in a specific ecosystem should be taken into account when short-term accuracy is required to gain a mechanistic understanding of R_s dynamics, to forecast the seasonality and diurnal course of R_s, and to fill gaps in an R_s time series 6]. For example, eddy-covariance studies have demonstrated that using moving-window approaches (i.e., local fitting) to model the seasonality in the temperature sensitivity and thus the seasonal evolution of R_e usually obtain better estimations than using a single, fixed annual function 20]. In addition, the use of variable, biophysically-controlled Q_{10} estimates has the potential to reproduce seasonal hysteresis in the R_s–T_s relationship, whereas a fixed annual parameter induces seasonal R_s biases (Fig. 2, 3).

Another important factor in choosing the proper Q_{10} implementation is the level at which respiratory CO_2 release is simulated. An ecosystem-specific empirical temperature response model which treats R_s or R_e as a composite flux (e.g., combining autotrophic and heterotrophic components) or as an emergent system behavior should adopt the apparent temperature response function because all effects on respiration, including those of confounding factors (e.g., plant phenology), have been implicitly incorporated into the model. In contrast, a process-based, bottom-up model, which explicitly simulates the mechanisms of different respiration components and their driving factors, should be parameterized with unconfounded short-term Q_{10} values for each component.

Lastly, previous studies 3] and our results imply that ecosystem carbon models should take into account the within-stand spatial uncertainty of temperature response parameters (e.g., as a function of their magnitudes, Fig. 4), rather than merely using a spatially deterministic value.

Acknowledgments

We thank Xiaomin Bai, Zheng Wei, Xiang Tang and Ben Wang for their assistance with the field measurements and instrumentation maintenance. We are grateful to the two anonymous reviewers and the Academic Editor for providing insightful comments and suggestions. We also thank Dr. Alan

Barr for his help with language revision, and valuable comments on the manuscript.

Author Contributions

Conceived and designed the experiments: TZ BW XW GH. Performed the experiments: XJ WC HY GH. Analyzed the data: XJ TZ WC. Wrote the paper: XJ TZ BW YZ.

References

1. Yu X, Zha T, Pang Z, Wu B, Wang X, et al. (2011) Response of soil respiration to soil temperature and moisture in a 50-year-old oriental arborvitae plantation in China. PLoS ONE 6: e28397.
2. Gaumont-Guay D, Black TA, Griffis TJ, Barr AG, Jassal RS, et al. (2006) Interpreting the dependence of soil respiration on soil temperature and water content in a boreal aspen stand. Agric For Meteorol 140: 220–235.
3. Xu M, Qi Y (2001) Spatial and seasonal variations of Q_{10} determined by soil respiration measurements at a Sierra Nevadan forest. Global Biogeochem Cycles 15: 687–696.
4. Sampson DA, Janssens IA, Curiel Yuste J, Ceulemans R (2007) Basal rates of soil respiration are correlated with photosynthesis in a mixed temperate forest. Glob Chang Biol 13: 2008–2017.
5. Bond-Lamberty B, Thomson A (2010) Temperature-associated increases in the global soil respiration record. Nature 464: 579–582.
6. Janssens IA, Pilegaard K (2003) Large seasonal changes in Q_{10} of soil respiration in a beech forest. Glob Chang Biol 9: 911–918.
7. Mahecha MD, Reichstein M, Carvalhais N, Lasslop G, Lange H, et al. (2010) Global convergence in the temperature sensitivity of respiration at ecosystem level. Science 329: 838–840.
8. Tang J, Baldocchi DD, Xu L (2005) Tree photosynthesis modulates soil respiration on a diurnal time scale. Glob Chang Biol 11: 1298–1304.
9. Vargas R, Baldocchi DD, Allen MF, Bahn M, Black TA, et al. (2010) Looking deeper into the soil: biophysical controls and seasonal lags of soil CO_2 production and efflux. Ecol Appl 20: 1569–1582.
10. Phillips CL, Nickerson N, Risk D, Bond BJ (2011) Interpreting diel hysteresis between soil respiration and temperature. Glob Chang Biol 17: 515–527.
11. Curiel Yuste J, Janssens IA, Carrara A, Ceulemans R (2004) Annual Q_{10} of soil respiration reflects plant phenological patterns as well as temperature sensitivity. Glob Chang Biol 10: 81–94.
12. Wang X, Piao S, Ciais P, Janssens IA, Reichstein M, et al. (2010) Are ecological gradients in seasonal Q_{10} of soil respiration explained by climate or by vegetation seasonality?. Soil Biol Biochem 42: 1728–1734.
13. Chen H, Tian HQ (2005) Does a general temperature-dependent Q_{10} model of soil respiration exist at biome and global scale? J Integr Plant Biol 47: 1288–1302.
14. Zheng ZM, Yu GR, Fu YL, Wang YS, Sun XM, et al. (2009) Temperature sensitivity of soil respiration is affected by prevailing climatic conditions and soil organic carbon content: A trans-China based case study. Soil Biol Biochem 41: 1531–1540.
15. Savage K, Davidson EA, Richardson AD, Hollinger DY (2009) Three scales of temporal resolution from automated soil respiration measurements. Agric For Meteorol 149: 2012–2021.
16. Vargas R, Detto M, Baldocchi DD, Allen MF (2010) Multiscale analysis of temporal variability of soil CO_2 production as influenced by weather and vegetation. Glob Chang Biol 16: 1589–1605.
17. Li H, Yan J, Yue X, Wang M (2008) Significance of soil temperature and moisture for soil respiration in a Chinese mountain area. Agric For Meteorol 148: 490–503.
18. Tian DL, Wang GJ, Yan WD, Xiang WH, Peng CH (2010) Soil respiration dynamics in *Cinnamomum camphora* forest and a nearby *Liquidambar formosana* forest in Subtropical China. Chin Sci Bull 55: 736–743.
19. Cao J (2011) Above- and belowground carbon pools in different ages of Chinese pine and oriental arborvitae plantation forests in northern mountain areas of Beijing [Ph.D. thesis]: Beijing Forestry University.
20. Moffat AM, Papale D, Reichstein M, Hollinger DY, Richardson AD, et al. (2007) Comprehensive comparison of gap-filling techniques for eddy covariance net carbon fluxes. Agric For Meteorol 147: 209–232.
21. Lloyd J, Taylor JA (1994) On the temperature dependence of soil respiration. Funct Ecol 8: 315–323.
22. Niu S, Luo Y, Fei S, Montagnani L, Bohrer G, et al. (2011) Seasonal hysteresis of net ecosystem exchange in response to temperature change: patterns and causes. Glob Chang Biol 17: 3102–3114.
23. Gaumont-Guay D, Black TA, Barr AG, Jassal RS, Nesic Z (2008) Biophysical controls on rhizospheric and heterotrophic components of soil respiration in a boreal black spruce stand. Tree Physiol 28: 161–171.
24. Drewitt GB, Black TA, Nesic Z, Humphreys ER, Jork EM, et al. (2002) Measuring forest floor CO_2 in a Douglas-fir forest. Agric For Meteorol 110: 299–317.
25. Boone RD, Nadelhoffer KJ, Canary JD, Kaye JP (1998) Roots exert a strong influence on the temperature sensitivity of soil respiration. Nature 396: 570–572.
26. Cable JM, Barron-Gafford GA, Ogle K, Pavao-Zuckerman M, Scott RL, et al. (2012) Shrub encroachment alters sensitivity of soil respiration to temperature and moisture. J Geophys Res 117: G01001.
27. Goulden ML, Wofsy SC, Harden JW, Trumbore SE, Crill PM, et al. (1998) Sensitivity of boreal forest carbon balance to soil thaw. Science 279: 214–217.
28. Morén AS, Lindroth A (2000) CO_2 exchange at the floor of a boreal forest. Agric For Meteorol 101: 1–14.
29. Xu M, Qi Y (2001) Soil-surface CO_2 and its spatial and temporal variations in a young ponderosa pine plantation in northern California. Glob Chang Biol 7: 667–677.
30. Reichstein M, Falge E, Baldocchi D, Papale D, Aubinet M, et al. (2005) On the separation of net ecosystem exchange into assimilation and ecosystem respiration: review and improved algorithm. Glob Chang Biol 11: 1424–1439.
31. Atkin OK, Bruhn D, Hurry VM, Tjoelker MG (2005) *Evans Review No. 2*: The hot and the cold: unravelling the variable response of plant respiration to temperature. Funct Plant Biol 32: 87–105.
32. Bhupinderpal-Singh, Nordgren A, Löfvenius MO, Högberg MN, Mellander PE, et al. (2003) Tree root and soil heterotrophic respiration as revealed by girdling of boreal Scots pine forest: extending observations beyond the first year. Plant Cell Environ 26: 1287–1296.
33. Tang J, Baldocchi DD (2005) Spatial-temporal variation in soil respiration in an oak-grass savanna ecosystem in California and its partitioning into autotrophic and heterotrophic components. Biogeochemistry 73: 183–207.
34. Buchmann N (2000) Biotic and abiotic factors controlling soil respiration rates in *Picea abies* stands. Soil Biol Biochem 32: 1625–1635.
35. Adachi M, Bekku YS, Konuma A, Kadir WR, Okuda T, et al. (2005) Required sample size for estimating soil respiration rates in large areas of two tropical forests and of two types of plantation in Malaysia. For Ecol Manage 210: 455–459.
36. Davidson EA, Belk E, Boone RD (1998) Soil water content and temperature as independent or confounded factors controlling soil respiration in a temperate mixed harwood forest. Glob Chang Biol 4: 217–227.